



# Hierarchical control of DC micro-grid for photovoltaic EV charging station based on flywheel and battery energy storage system

Lei Shen<sup>a,\*</sup>, Qiming Cheng<sup>a</sup>, Yinman Cheng<sup>b,c</sup>, Lin Wei<sup>a</sup>, Yujiao Wang<sup>a</sup>

<sup>a</sup> College of Automation Engineering, Shanghai University of Electric Power, Shanghai 200090, China

<sup>b</sup> North Power Supply Branch, Shanghai Electric Power Company, Shanghai 200041, China

<sup>c</sup> College of Electronics and Information Engineering, Tongji University, Shanghai 201804, China

## ARTICLE INFO

### Keywords:

EV charging station  
DC-micro-grid  
Hierarchical control  
Energy storage  
Photovoltaic  
Flywheel

## ABSTRACT

For micro-grid systems dominated by new energy generation, DC micro-grid has become a micro-grid technology research with its advantages. In this paper, the DC micro-grid system of photovoltaic (PV) power generation electric vehicle (EV) charging station is taken as the research object, proposes the hybrid energy storage technology, which includes flywheel energy storage and battery energy storage. Flywheel energy storage is used to stabilize high frequency power fluctuations and some low frequency power. Lithium iron phosphate (LiFePO<sub>4</sub>) battery is used for balancing the reference power to maintain the DC bus voltage balance. Composition of the DC micro-grid and various operating modes are analyzed, a hierarchical coordinated control based on the power monitoring steps of the 5-layer DC bus voltage is proposed. Finally, simulation analysis is carried out on the MATLAB/Simulink software platform. Under different working states such as PV input power change, AC and DC loads change, EV charging condition change, and battery over-discharge, the proposed control strategy can make the DC bus voltage at different voltage layers effectively switch, and keep the DC bus voltage balance, thus to achieve flexible and reliable operation of the DC micro-grid system.

## 1. Introduction

### 1.1. Motivation

Distributed generation (DG) system with renewable energy as its main component is connected to the large power grid, which will affect the power quality of the power system. The micro-grid constructed by distributed energy and load can satisfy demand of local users for power quality and power supply security, and at the same time, it can reduce the impact of a large number of distributed power infiltration on the power system [1,2].

Many DGs and energy storage devices exist in the form of DC output, such as PV power generation system, fuel cell, storage battery, super-capacitor, etc. Especially solar energy is widely distributed, clean and pollution-free, and it is internationally recognized as an ideal alternative energy source. With the wide development and popularization of electric vehicles (EVs) in the world, the local absorption of photovoltaic (PV) energy in the form of micro-grid charging stations is a direct and effective way to achieve low carbon [3,4].

Compared with AC micro-grid, DC micro-grid can reduce the number of DC/AC converter in equipment, and it is easy to coordinate

control between micro-grid sources. Power balance between power-source supply and load can be achieved by controlling the stability of DC bus voltage. There are no problems in DC micro-grid, such as frequency and power angle stability, reactive power circulation, etc. In the micro-grid system dominated by new energy generation, DC micro-grid is an ideal solution.

### 1.2. Literature survey

The introduction of EVs and distributed renewable resources (DRRs) into the micro-grid is aimed at achieving the three most critical goals of the century: the use of environmentally friendly energy, reliable supply of load demand and sustainable development of power systems. The smart micro-grid and its role in future power systems were introduced in study [5], including the study of multiple grid architectures and control schemes. And through the evaluation of load and resource priority, the load and energy distribution and the hierarchical method based on Frank Wolf algorithm and Danzig Wolff decomposition are used to solve the large-scale economic dispatch problem of smart grid and so on. In study [6], a novel method for simultaneous allocation of DRR and EV parking lots is proposed. This synchronization method will

\* Corresponding author.

E-mail address: [shdl\\_shenlei@163.com](mailto:shdl_shenlei@163.com) (L. Shen).

<https://doi.org/10.1016/j.epsr.2019.106079>

Received 20 November 2018; Received in revised form 4 October 2019; Accepted 15 October 2019

Available online 13 November 2019

0378-7796/ © 2019 Elsevier B.V. All rights reserved.

certainly improve the performance of smart distribution network, thereby achieving the best level of loss reduction, involving the decision-making factors of the parking lot investors and the constraints of the distribution network.

In recent years, there have been preliminary theoretical studies on the structure, operation mode and control method of DC micro-grid [7,8]. On the one hand, there are many controllable units in the micro-grid and they are scattered. In order to ensure their reliable and stable operation, under different operating conditions and load switching, the hierarchical coordinated control of power electronic converters needs to be further studied. On the other hand, the energy sources in micro-grid, such as PV and wind power, have obvious intermittence, so increasing energy storage system is very important to maintain system stability, but it is difficult for a single energy storage device to meet both power and energy requirements [9–11].

At present, there are many studies on hybrid energy storage system composed of super-capacitors and batteries to suppress power and energy fluctuations [12–15]. However, super-capacitors have some shortcomings, such as low energy storage density, improper installation location or use, which can lead to electrolyte leakage and high price. Compared with super-capacitor energy storage, flywheel energy storage has great advantages in power quality, frequency support, load change and so on [16–18]. Hybrid energy storage system is ideal for smooth control of DC bus voltage [19,20].

### 1.3. Contribution

This paper proposes a DC micro-grid coordinated control technology for EV charging station based on hybrid energy storage. The hybrid energy storage includes mixed energy storage of flywheel and battery, and designed a five-layer voltage coordinated control strategy for DC bus. The coordinated control of PV power generation, EVs charging and discharging, and load power demand in the micro-grid system is realized. The proposed control strategy was simulated and analyzed on Matlab software platform. There are three main contributions to this article:

- The paper proposes a basic framework based on photovoltaic power generation hybrid energy storage electric vehicle DC micro-grid, which has universality, can absorb new energy and grid connection well.
- In the hybrid energy storage strategy, the flywheel is used to smooth high frequency power fluctuations and some low frequency power, the battery is used to balance the reference power to maintain the bus voltage smooth and stable, which can improve the power quality of the micro-grid system.
- Set a higher level power monitoring to improve control performance and increase control flexibility.

### 1.4. Organization of the paper

The rest of this paper is organized as follows: Firstly, the structure of charging station is introduced, and the mathematical principles of photovoltaic power generation system, LiFePO<sub>4</sub> battery and flywheel hybrid energy storage system are analyzed. Secondly, combined with the coordinated control of flywheel and battery in hybrid energy storage system, a hierarchical coordinated control scheme based on five-layer DC bus voltage is proposed, and the power monitoring steps are given. Finally, the charging station simulation system is established by Matlab/Simulink, and the charging station under different conditions is simulated and verified.

## 2. Charging station DC micro-grid

The DC micro-grid PV charging station designed in this paper is shown in Fig. 1. It is mainly composed of PV power generation system,

hybrid energy storage, EV charging and discharging system, DC/DC and AC/DC converter, AC and DC loads and central control unit, and common DC bus. In the PV charging station system, EV can not only absorb energy from the grid as a load on the grid; it also feeds back energy to the grid to improve the operational reliability of the grid, thus fully utilizing the energy storage of the EV.

The micro power supply, energy storage devices, and loads in the system are connected to the DC bus through corresponding converters. The DC bus voltage is designed to be 600 V and the AC bus voltage is 380 V. PV charging station is mainly operated in a DC micro-grid structure, and a hybrid energy storage system is formulated to coordinate and optimize the energy configuration of the micro-grid, to realize coordinated control of PV power generation and EV charging and discharging. And PV charging station can change work mode between on-grid and off-grid, through a Solid State Switch (SST).

Among the composition of charge station:

- (1) PV power generation system is composed of PV array and unidirectional DC/DC converter, and maximum power point tracking (MPPT) is realized by perturbation and observation (P&O) method.
- (2) Hybrid energy storage system consists of battery and flywheel energy storage. Because of the intermittence and randomness of PV power generation, it is difficult for a single energy storage device to meet the requirements of power and energy at the same time. In hybrid energy storage mode, the battery is responsible for smoothing the low-frequency power component in the system, while the flywheel is responsible for compensating the high-frequency power component in the system, so as to meet the power quality and load demand of micro-grid operation. Energy storage system plays the role of smoothing power and energy demand and supporting DC bus voltage when operates in off-grid condition and charging and discharging when operates in on-grid condition.
- (3) DC/DC converters can be divided into unidirectional and bidirectional converters. The PV power generation can only use unidirectional energy flow. And energy storage and EV charging and discharging system need to use bidirectional control to realize the interaction between the two sides.
- (4) AC/DC converter includes AC/DC converter in flywheel system and AC/DC converter on network side. The former can be regarded as part of the flywheel energy storage system, and the latter can be used to connect the DC bus and the AC bus of the charging station. According to the energy demand of charging station, when charging station is connected to the grid, AC/DC converter on the grid side provides power and energy demand or absorbs excess power for charging station; when charge station operates under off-grid condition, AC/DC converter provides voltage and frequency support for AC side and supplies power.
- (5) Charging station loads are classified into AC and DC loads. Among them, the AC load is usually the constant power type and used under the traditional metropolis power. The DC load is usually the constant resistance type and suitable for the DC voltage.
- (6) The central control unit is responsible for the monitoring and control of each unit, including the monitoring of voltage, current and energy, to achieve central control and coordinate the optimal operation of each component of the charging station.

### 2.1. PV Power Generation System

4 basic parameters of the PV cell, short circuit current  $I_{sc}$ , open circuit voltage  $U_{oc}$ , maximum power voltage  $U_m$  and current  $I_m$ , can be provided by the manufacturer while in the practical application, which are measured under the standard condition with temperature  $T_{ref} = 25^\circ\text{C}$ , light intensity  $S_{ref} = 1000\text{ W/m}^2$ , and spectrum  $AM = 1.5$ . From the output characteristic  $U$ - $I$  relation of the PV semiconductor device, the basic equation of the output current is [2]:

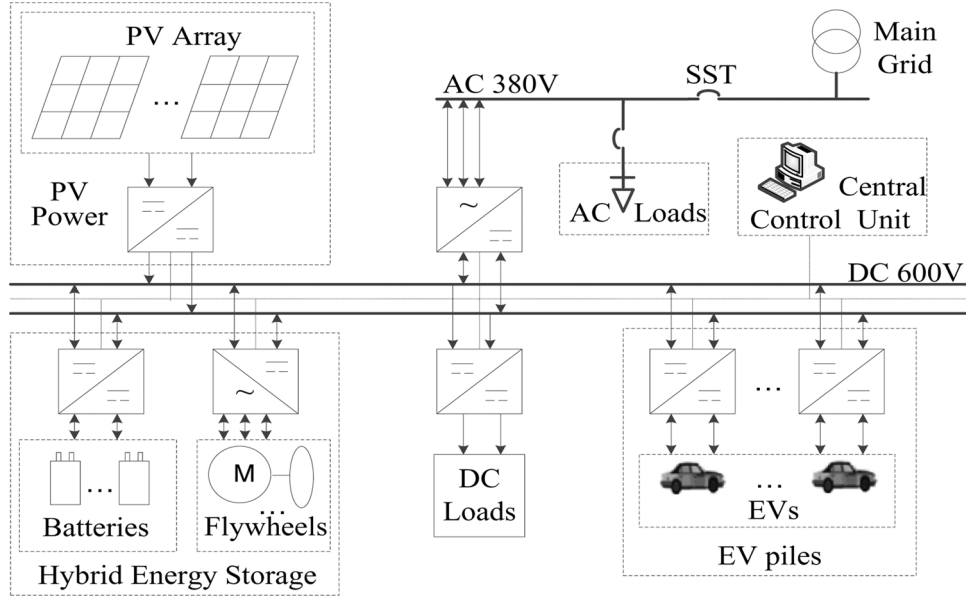


Fig. 1. Micro-grid structure of PV-based EV charging station with energy storage.

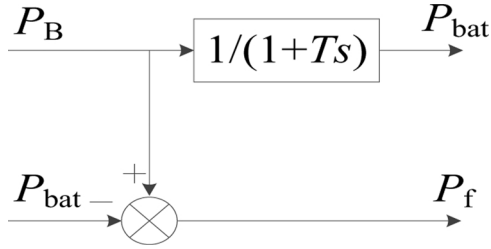


Fig. 2. Smooth control structure of the hybrid energy storage.

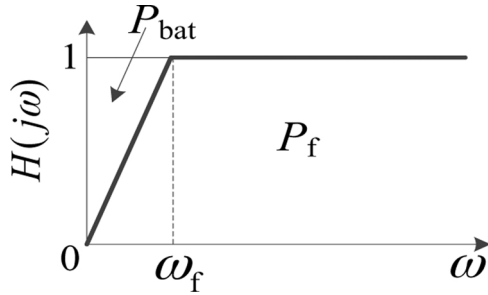


Fig. 3. Bode diagram of output power transfer function of flywheel and battery.

$$C_1 = (1 - I_m/I_{sc})e^{-U_m/(C_2 U_{oc})} \quad (2)$$

$$C_2 = (U_m/U_{oc} - 1)[\ln(1 - I_m/I_{sc})]^{-1} \quad (3)$$

where  $U$  is the output voltage (V),  $I$  is the output current (A),  $C_1$ ,  $C_2$  refer to correction factors of current, voltage, respectively. With the effect of changes in solar radiation and temperature considered, it becomes:

$$I = I_{sc}[1 - C_1(e^{(U-dU)/(C_2 U_{oc})} - 1)] + dI \quad (4)$$

$$dI = I_{sc}[\frac{aS}{1000}(T - 25) + (\frac{S}{1000} - 1)] \quad (5)$$

$$dU = -bU_{oc}[T - 25] - R_0 dI \quad (6)$$

where  $S$  is the actual light intensity ( $W/m^2$ ),  $T$  is the actual temperature ( $^{\circ}C$ ),  $R_0$  is the equivalent series resistance ( $\Omega$ ), and  $a$ ,  $b$  refer to the current compensation factor ( $A/^{\circ}C$ ), voltage compensation factor ( $V/^{\circ}C$ ), respectively.

Then, the  $I$ - $U$  and  $P$ - $U$  features of PV cells can be obtained from Eq. (4) and  $P = IU$ .

## 2.2. Units of Hybrid Energy Storage System

LiFePO<sub>4</sub> battery has gradually become a large-scale application in the power and energy storage devices, the discharge voltage from the analysis of the discharge curve is [3]:

$$I = I_{sc}[1 - C_1(e^{U/(C_2 U_{oc})} - 1)] \quad (1)$$

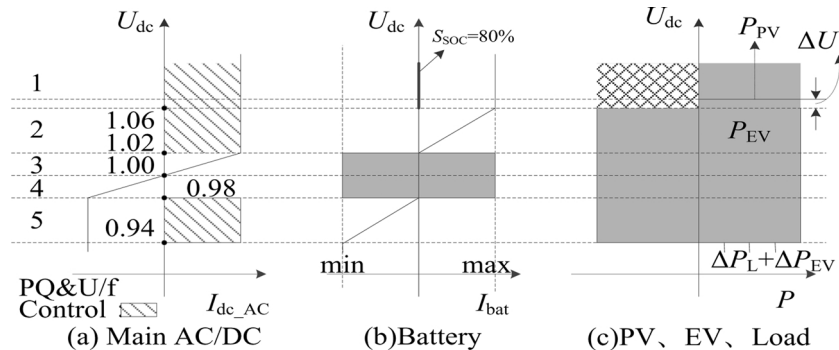


Fig. 4. Hierarchical control strategy of DC voltage.

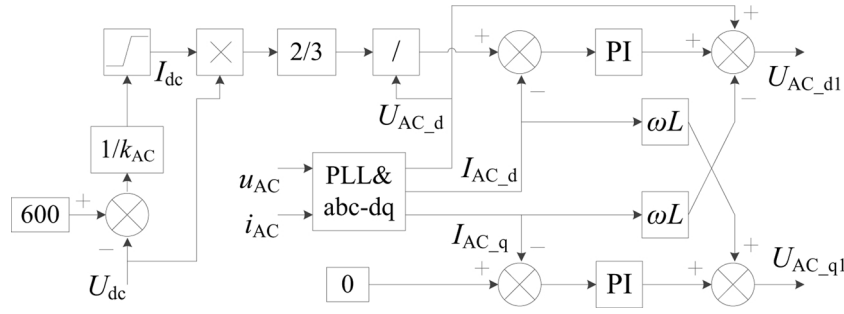


Fig. 5. Control structure of the main AC/DC converter in the micro-grid.

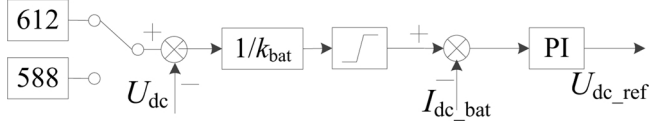


Fig. 6. DC/DC control structure of battery energy storage.

$$U_{bat} = E_0 - K \frac{Q}{Q - it} \cdot it - K \frac{Q}{Q - it} \cdot i^* + A \cdot \exp(-B \cdot it) - R_0 \cdot i \quad (7)$$

where  $E_0$  is the battery constant voltage (V),  $K$  is the polarization voltage (V),  $Q$  is the battery capacity (Ah),  $it$  is the actual battery discharge (Ah),  $i$  is the battery current (A),  $A$  is the exponential zone amplitude (V),  $B$  is the exponential zone time constant inverse (Ah)<sup>-1</sup>,  $i^*$  refers to the battery current after the first-order low-pass filter (A) in order to avoid the algebraic loop problem.

The charge voltage of battery is:

$$U_{bat} = E_0 - K \frac{Q}{it + 0.1 \cdot Q} \cdot i^* - K \frac{Q}{Q - it} \cdot it + A \cdot \exp(-B \cdot it) - R_0 \cdot i \quad (8)$$

Then, the model of LiFePO<sub>4</sub> battery can be established with the

battery State-Of-Charge (SOC) as only one state variable.

Lithium battery is an energy storage device with a small power range, slow rate for storage/release, and limited life, whose compensation is mainly for the low frequency fluctuation of the system power component. In the meantime, by contrast, flywheel energy storage is of large power range, fast storage/release rate, near-infinite cycle number, and considerable capacity, so that it mainly used for the compensation of high frequency power component [13].

Flywheel energy storage system generally consists of the flywheel rotor, drive motor, the vacuum chamber, bearings, power electronics converter and control system. The rotor of flywheel is coaxial with the drive motor, so it can be seen as a mass attached to the shaft of the drive motor [18].

A permanent magnet synchronous motor (PMSM) is regarded as a flywheel energy storage required in this article, the electromagnetic torque equation of which is:

$$T_e = 1.5p[\lambda i_q + (L_d - L_q)i_d i_q] \quad (9)$$

where  $i_d$ ,  $i_q$  are the stator current of d, q axis component, respectively.  $L_d$ ,  $L_q$  refer to the stator winding equivalent inductance of d, q axis, respectively, and  $\lambda$  is the permanent magnet rotor flux linkage,  $p$  is the

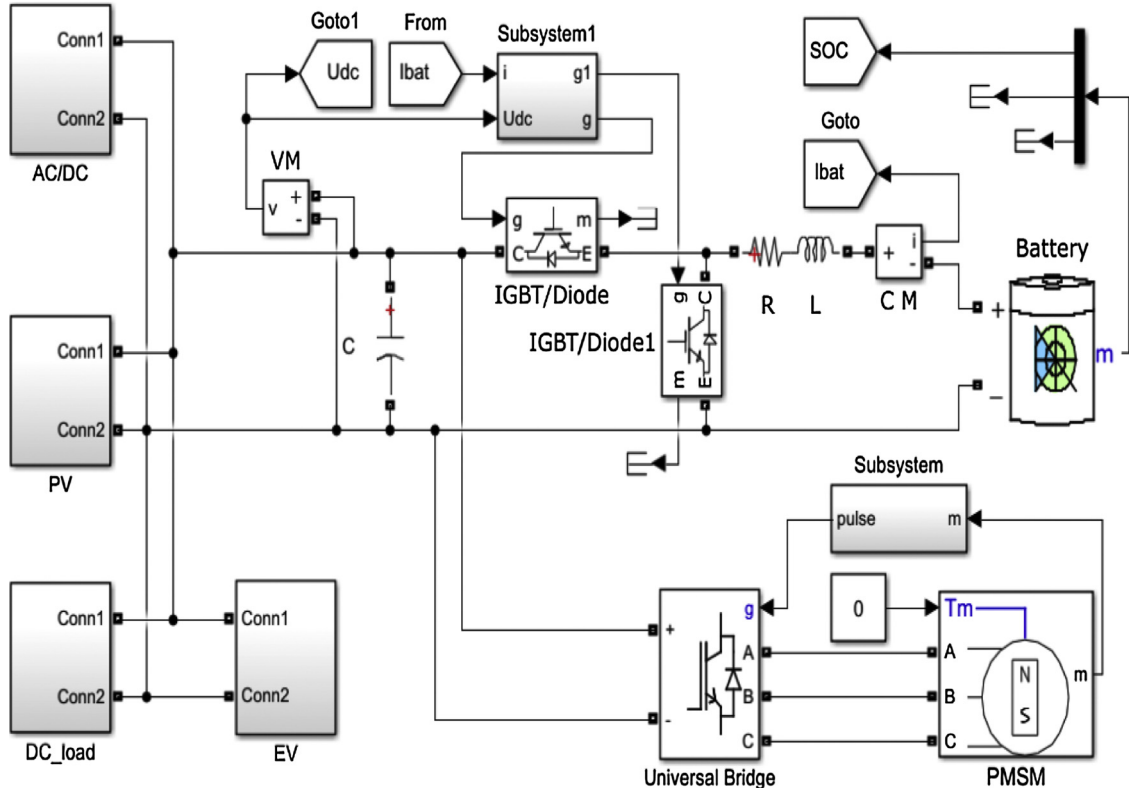


Fig. 7. PV hybrid energy storage EV charging station schematic overview.

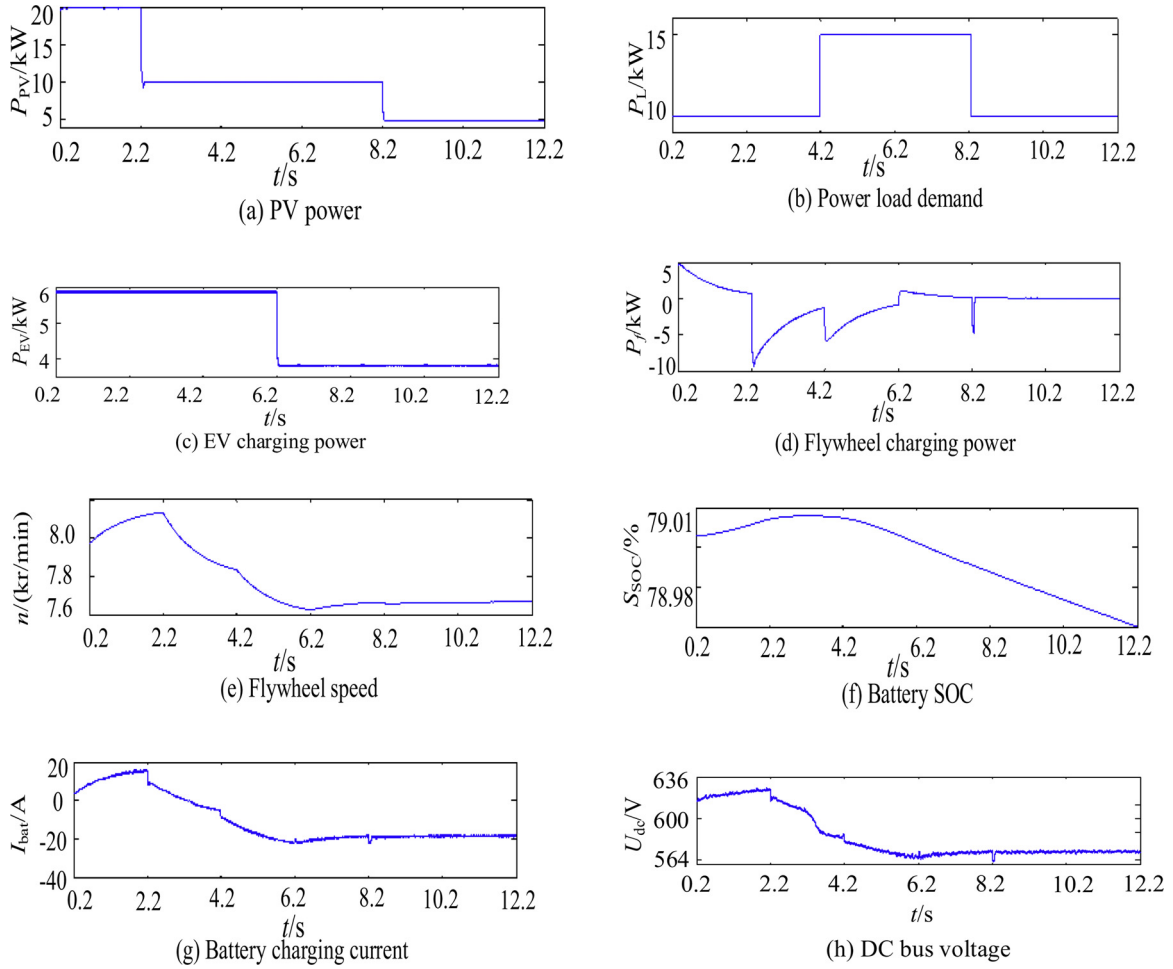


Fig. 8. System operating characteristics off-grid in general.

number of pole-pairs.

If the loss of motor electromagnetic power has been neglected, the power output is equal to electromagnetic power of the motor, and let  $L_d = L_q$ , the storing power of the flywheel will be:

$$P_f = 1.5p\lambda i_q \omega_r \quad (10)$$

where  $\omega_r$  is the mechanical angular velocity of the rotor.

The power storage/release control of the flywheel can be realized by controlling the motor speed change based on the q-axis current reference signal of the flywheel stator, which is coming from the power input reference signal while the rotor speed has been known, according to formula (10).

### 3. Hierarchical control strategy

#### 3.1. Hierarchical control of the hybrid energy storage system

This paper uses the way combination of the flywheel and battery energy storages as a hybrid energy storage, where the flywheel energy storage compensating high frequency and part of the low-frequency power for the smooth of the battery energy storage power input, while battery maintain smooth the stability of the DC bus voltage, so that to improve the power quality and prolong the service life of the batteries.

The hierarchical control strategy of the hybrid energy storage system is shown in the Fig. 2, as can be seen there is a low-pass filter to separate the different frequencies of charging power borne by the flywheel and battery energy storages respectively. Where,  $P_b$  is the charging power of the hybrid energy storage system,  $P_f$  and  $P_{bat}$  are the

charging power of the flywheel and battery energy storage respectively, and  $T$  is the time constant of the first-order low-pass Butterworth filter.

Fig. 3 shows the Bode diagram of the power output transfer function of flywheel and battery energy storage, where  $\omega_f$  is the angular frequency under filter time constant  $T$ .

As can be seen from Figs. 2 and 3, the value of  $P_f$  is 1 when the angular frequency is greater than  $\omega_f$ , and it becomes proportional to the angular frequency when the angular frequency is greater than 0 and less than  $\omega_f$ , which means the flywheel energy storage can compensate power output power of all high frequency power component fluctuation greater than  $\omega_f$  angular frequency, and share part of low frequency. As a result, the flywheel and battery energy storage share the power needed in the system, achieving the balance of power flowing among the DC bus.

#### 3.2. Operation modes of micro-grid

##### 3.2.1. Off-grid mode

When the micro-grid is running on the off-grid mode, the AC bus acts as an AC load which is supplied by the DC bus, by this time, the battery energy storage maintains the power balance of the DC bus for the voltage support, with equation as follows:

$$P_{bat} = P_{PV} - P_{DL} - P_{AL} - P_{EV} - P_f \quad (11)$$

where,  $P_{EV}$  is the charging power of EVs,  $P_{PV}$  is the PV generating power,  $P_{DL}$ ,  $P_{AL}$  refer to the load power of the DC, AC side, respectively.

As is known, the charging/discharging of EVs is random and schedulable. In the case of the power from energy storage system is



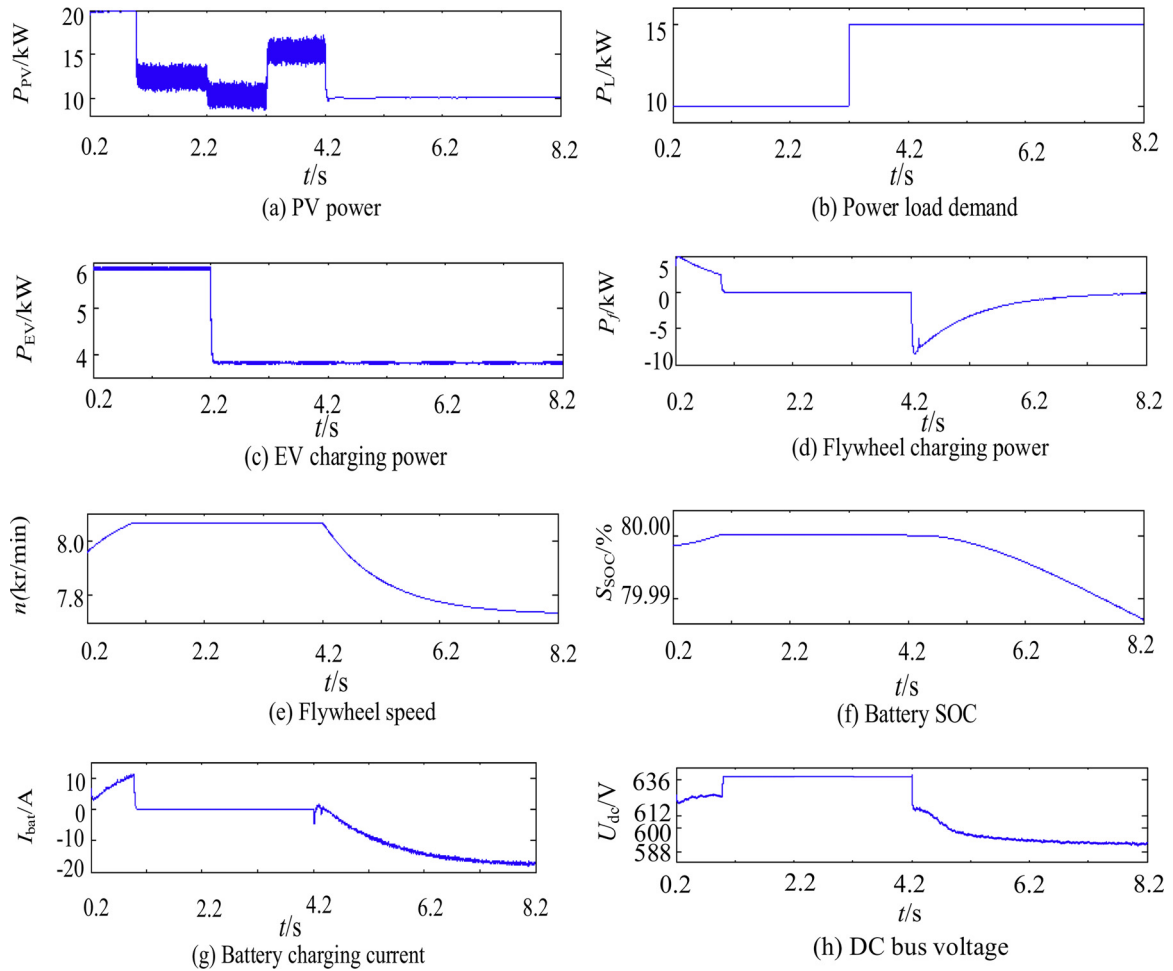


Fig. 9. System operating characteristics off-grid with battery energy storage fully charged.

insufficient, so it can be through the control of EVs charging/discharging for the power supplement required to reduce to power output of the energy storage system, thus maintain the stability of the DC bus voltage. But the most direct way to maintain the power balance in an adjustable range provided by the energy storage system, is via the removal of the loads, which can be divided into important and secondary ones to ensure the reliability and flexibility of system after cutting off in order.

In the case of power into energy storage system is abundant, the energy storage power input should be reduced to maintain the power balance for a stable bus voltage, by the means of changing the working mode of the PV array converter into constant voltage control (CVC) mode [7]. It will reduce the PV power input, i.e.:

$$P_{PV} - \Delta P_{PV} = P_{DL} + P_{AL} + P_{EV} + P_B \quad (12)$$

Where,  $\Delta P_{PV}$  is the reduced PV power input for the DC bus power balance.

### 3.2.2. On-grid mode

When micro-grid is on-grid, the AC bus is connected to the power system major grid, the stability of the DC bus voltage can be supported by the major grid through the main bi-directional AC/DC from AC-side. The power exchanged to AC bus from DC bus can be:

$$P_{AC} = P_{PV} - P_{DL} - P_{AL} - P_{EV} - P_B \quad (13)$$

where,  $P_{AC}$  is the power into AC bus provided by DC-side.

The charging or discharging of EVs and energy storage can be dispatched in a permissible range for the frequency and peak load regulation of the major grid, however, it will be limited by the capacity of

the main AC/DC converter that the power exchange between DC bus and AC bus in the process of actual operation. When the main AC/DC has reached the power limit, it will enter the constant power control, and lost the ability of voltage regulation. At this point, the AC bus will be equal to a constant power load or supply, and the energy storage system will maintain the balance of DC bus power, as follows:

$$P_B = P_{PV} - P_{DL} - P_{AL} - P_{EV} - P_{AC} \quad (14)$$

Corresponding countermeasures the same as off-grid, when the required power is beyond the adjustment range of the energy storage system.

### 3.3. Hierarchical control of DC bus voltage

In the DC micro-grid, the voltage of DC bus is the only indicator reflects the power balance in the system. The corresponding voltage point of power balance varies under different modes of system operation, so the voltage hierarchical control can be used to achieve co-ordinated optimization of power allocation in the DC micro-grid. The hierarchical control strategy of DC bus voltage is shown in Fig. 4, in which (a)–(c) refer to voltage control characteristics under different layers of the main AC/DC charging power to AC-side, battery energy storage charging power, PV power generation with EV charging power and Load lightening power, respectively. The basic value DC bus voltage is set at 600 V, and each reference voltage point set with per unit in Fig. 4.

As can be seen from Fig. 4, in this paper, the DC bus voltage hierarchical control is designed to 5 layers, each one possesses

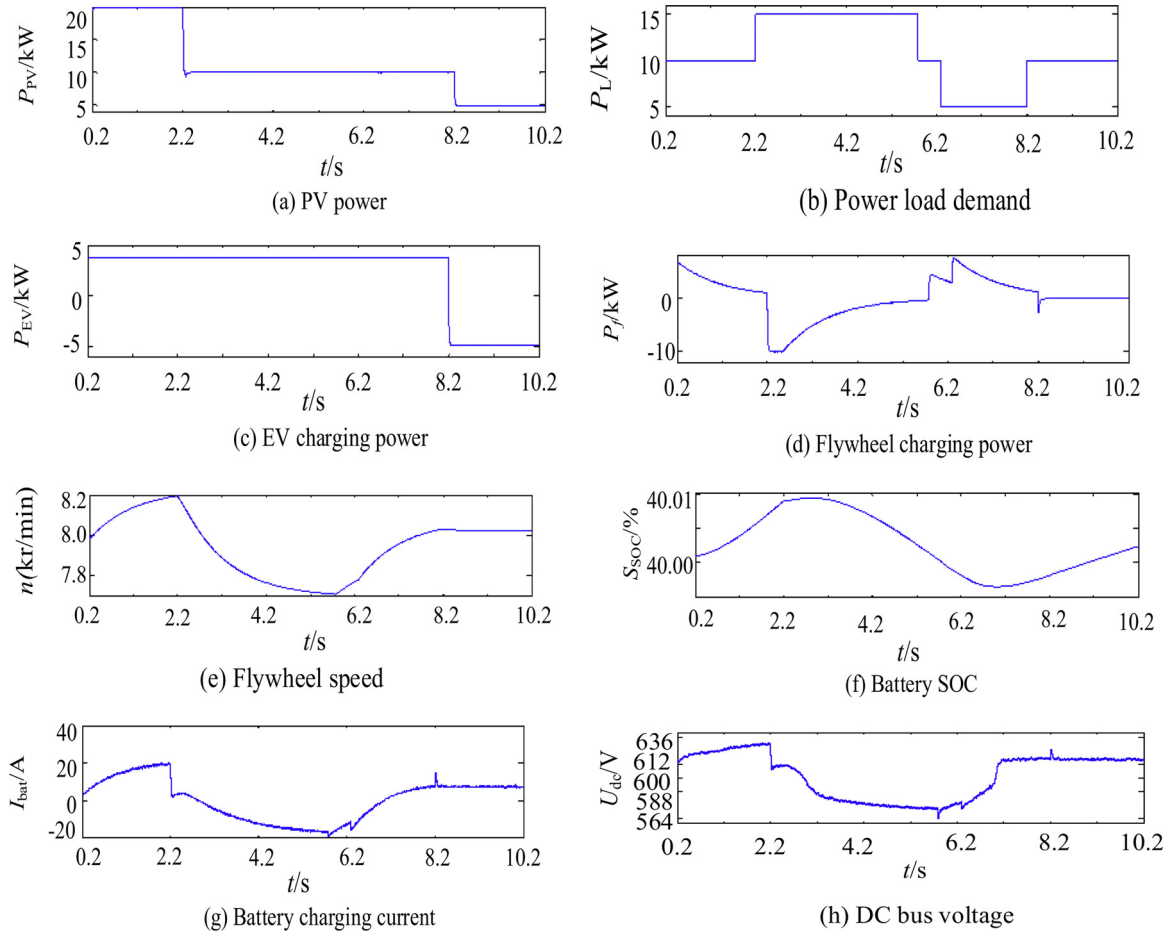


Fig. 10. System operating characteristics off-grid with battery energy storage excessive discharged.

corresponding voltage droop control of converter, to ensure the power balance. According to the location of the DC bus voltage in different layers, the system working mode can be determined for corresponding control of converters connected with DC bus without any communication. To avoid the frequent switching of working mode among 5 layers during the operation, a hysteresis control should be set for the select of voltage layer in the switch point. The details of hierarchical control are summarized as follows:

### 3.3.1. Control of the bidirectional AC/DC converter

#### a. Off-grid mode

When it works at off-grid mode, the U/f control will be used to control the bi-directional AC/DC converter, supports constant voltage and frequency for the AC bus. At this point, the AC bus is equal to the load, and should meet the demand of load lightening if the DC bus voltage is going to be lower than the 5th layer as the lack of power.

#### b. On-grid mode

According to the power conservation theorem, the current relationship between AC-side and DC-side is satisfied:

$$I_{AC\_d} = 2U_{dc}I_{dc\_AC}/3U_{AC\_d} \quad (15)$$

where,  $U_{AC\_d}$ ,  $I_{AC\_d}$  refer to d-axis component of AC-side voltage, current, respectively. The voltage control of DC bus can be realized through the AC-side d-axis current of bi-directional AC/DC converter, on the basis of Eq. (15).

The control of bi-directional AC/DC converter under the on-grid mode can be divided into two strategies, the one exports constant active and reactive power to the AC-side called PQ control, and the other supports voltage for DC bus shown in Fig. 5, where  $k_{AC}$  is the droop coefficient,  $L$  is the filter inductance in AC-side,  $U_{AC\_d1}$ ,  $U_{AC\_q1}$  refer to

control signal of voltage AC-side on d-axis, q-axis, respectively. As can be seen from Fig. 5, the outer-ring voltage droop control is adopted to realize to the stability of DC bus voltage, and the inner current control increase the response speed with decoupling of feedforward control. When the voltage is below the 3rd or higher than the 4th layer, the control shown in Fig. 5 can be regarded as a constant power control, similar with the PQ control.

### 3.3.2. Control of the converter of the battery energy storage

As is shown in Fig. 4(b), the hybrid energy storage system turns into a grid standby state on-grid when the DC bus voltage stays at the layer 3 and 4, charge or discharge in free and set aside. In order to ensure the adjustment ability of battery storage, this paper takes a constant current charge/discharge control to reach the target value 70% of remaining power for standby. As to flywheel, a constant power control is taken to reach 80% of remaining power for standby.

When the voltage of DC bus is in the rest layers, a maximum current limited droop control, namely double-loop control of voltage outer and current inner, will be used to control the battery bi-directional DC/DC for the DC bus voltage supporting. The control structure diagram of battery energy storage is shown in Fig. 6, where  $k_{bat}$  is the droop control coefficient,  $U_{dc\_ref}$  is the voltage control signal, 612, 588 refer to the actual voltage of per unit value 1.02, 0.98, respectively.

### 3.3.3. Hierarchical of PV, EV and load

When the DC bus voltage is at the first layer, the PV power exceeds the energy demand of the system, causing the DC bus voltage to rise. It is necessary to cut off part of the PV array power to maintain the stability of the system. Meanwhile, the PV array MPPT reduces the power to maintain the voltage stable. When the DC bus voltage is lower than

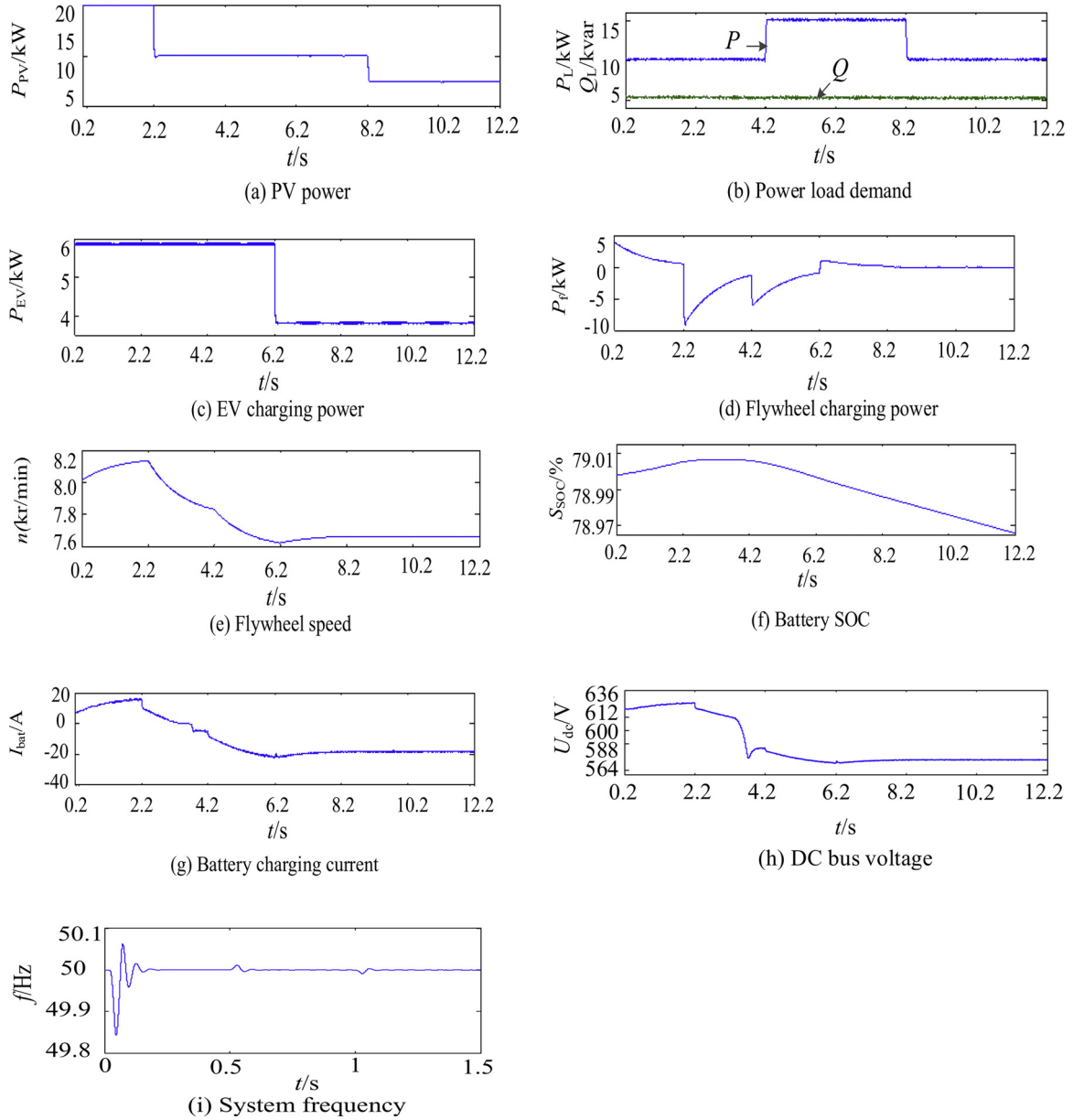


Fig. 11. System operating characteristics on-grid with PQ control in general.

the 5th layer, the load exceeds the energy supply of the system, causing the DC bus voltage to fall. It is necessary to cut off the load in order to ensure the voltage rise, and the power can be balanced by the bidirectional charge and discharge scheduling of the electric vehicle. In the first voltage layer, the EV only performs charging control; In other voltage layers, the EV performs bidirectional charging and discharging control according to requirements.

In this paper, the charging and discharging of EV adopt phased constant current control, that is to say the current amplitude decreases stepwise with the increase of the state of charge (SOC) of the EV battery. In order to characterize the charge and discharge characteristics of EV,  $P_{EV0}$  is the effective charging power of EV, and the charging efficiency of EV is:

$$\eta_{EV} = \frac{P_{EV0}}{P_{EV}} \quad (16)$$

Conversely,  $P_{EV0}$  becomes the EV discharge power, and  $P_{EV}$  the effective one, the discharge efficiency will be the inverse of  $\eta_{EV}$ .

### 3.3.4. Power monitor

An additional power monitor is used to achieve voltage transition more smooth in this paper, for the converter control strategy quickly switching among the hierarchical droop without any communication.

## 4. Simulation status

Taking the PV hybrid energy storage EV charging station shown in Fig. 7 as schematic overview of the paper, the system simulation is built based on Matlab/Simulink.

In order to validate the proposed hierarchical control strategy of EV charging station, simulation system has been built under the environment of MATLAB/Simulink software according to Fig. 1 structure. The parameters of the system are shown as follows:

- (1) The PV power  $P_{pv}$  is rated at 20 kW, and rated capacity of the bi-directional AC/DC converter  $P_{AL}$  is 30 kW. The PI regulator has a KP set to 0.8 and a KI set to 5 and time constant  $T = 1$  s.
- (2) LiFePO<sub>4</sub> battery voltage  $U_{ev0}$  rated at 360 V is used for EVs power,



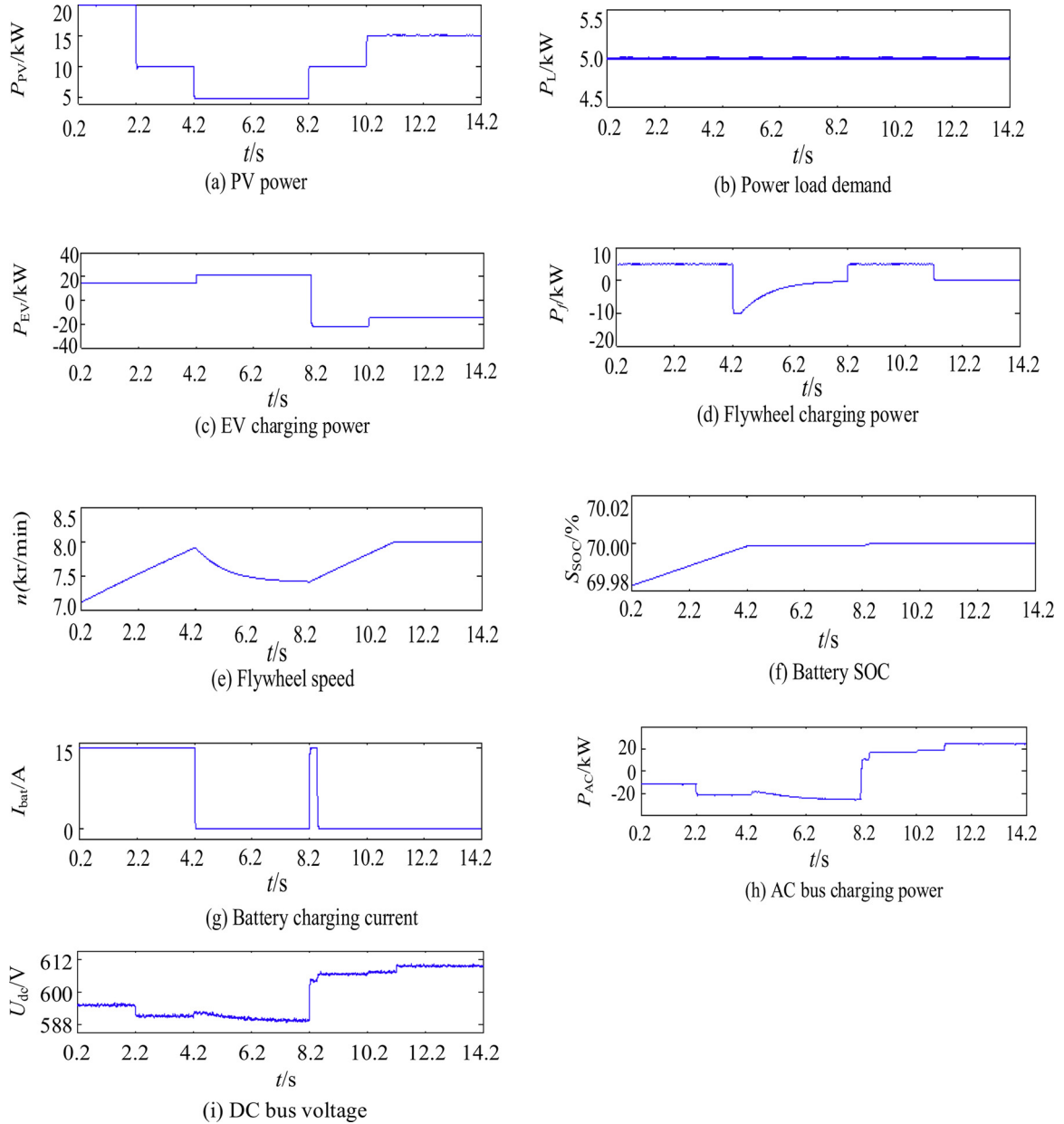


Fig. 12. System operating characteristics on-grid with hybrid energy storage charging.

and charge and discharge current uses 15 A and 10 A 2 modes for constant current charge and discharge. 4 EV piles is set in this system.

- (3) Battery energy storage system  $P_{bat}$ , with the same kind battery of EVs, is rated at 100 Ah, 20 kW, and adopt 0.15 C (15 A) constant current  $i_{AC}$  control for standby charging/ discharge on-grid.
- (4) The storage power of flywheel system  $P_f$  is 10 kW, the maximum speed  $n_{max}$  is 10000 r/min, minimum speed  $n_{min}$  5000 r/min.
- (5) A DC-side load constant power type  $P_{DL}$  L1, and two AC-side load  $P_{AL}$  constant power type load L2, L3, are allocated in the system, each rated at 5 kW, the priority level declines in turn.

#### 4.1. Off-grid

##### 4.1.1. Simulation in general pattern

Due to the system capacity restriction, only 1 EV pile works in the off-grid mode. As is shown in Fig. 7, at 0.2 s, the simulation begins with a 20 kW ( $P_{PV}$ ) PV power, L1 and L2 switched in as a total 10 kW ( $P_L$ )

load. The EV charge current is 15 A with effective charge power about 5.4 kW ( $P_{EV0}$ ). The storing power for flywheel ( $P_f$ ) declines gradually and the speed  $n$  rises with a reduced acceleration, which shows the remaining power from PV is being smooth transited into the battery energy storage. The DC bus voltage  $U_{dc}$  rises smooth and works at layer 2, with the battery charging current  $I_{bat}$  increases gradually. At 2.2 s, as  $P_{PV}$  reduced to 10 kW, the flywheel responds fast by change mode of discharge from charge, and gradually transits the power vacancy to the battery energy storage. The DC bus voltage reaches layer 5 across the 3rd and 4th layers.

At 4.2 s, load L3 is closed, and  $P_L$  becomes 15 kW. The DC bus voltage declines and continues to work on layer 5. At 6.2 s, the EV charge current is changed to 10 A, with  $P_{EV0}$  becomes 3.6 kW. Flywheel also is switched into the charge mode for the voltage smooth control of battery energy storage. At 8.2 s,  $P_{PV}$  is reduced to 5 kW, and L3 cleared as  $P_L$  changed 10 kW. A small current impact occurred and quickly disappeared in the system.

In off-grid mode, with the change of PV input power and system

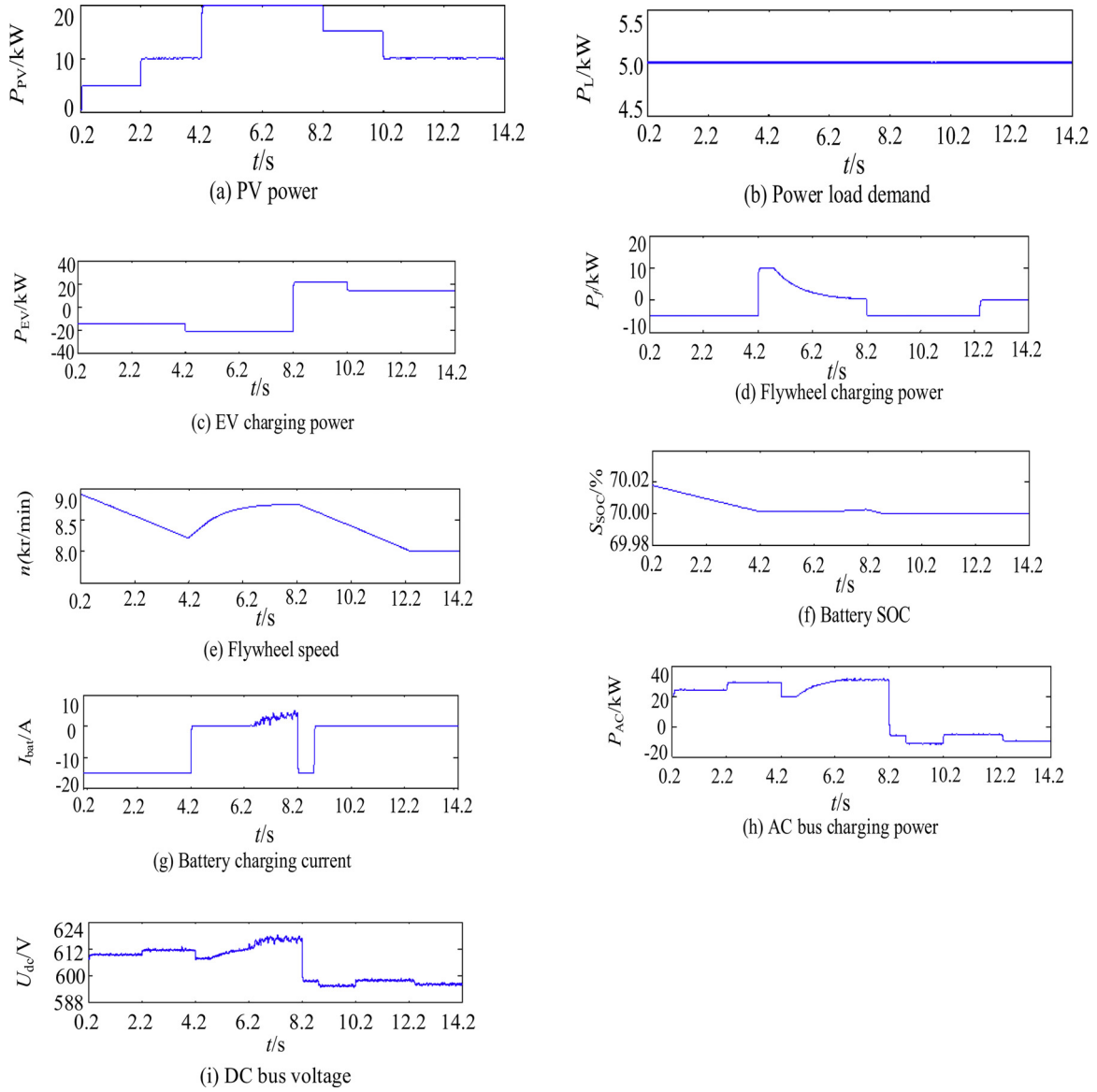


Fig. 13. System operating characteristics on-grid with discharging of the hybrid energy storage.

load, as well as the change of charging condition of EV, the power complementation of flywheel motor and battery in hybrid energy storage system can maintain the voltage balance in the second and fifth layers of the system well, and the transition is smooth and the effect is obvious.

#### 4.1.2. Simulation with battery energy storage fully charged

As is shown in Fig. 9, about at 1.2 s, the SOC of energy storage battery reaches 80%, and is ceased to be charged for protecting. The flywheel still maintains the speed standby. The voltage of DC bus rises into the layer 1, and becomes 639 V maintained by the CVC control of PV converter. At 2.2 s, PV power input is reduced to 10 kW, and flywheel jumps into discharging for power supplementary, and leads the voltage of DC bus  $U_{dc}$  to be gradually transited to the 5th layer supported by the battery energy storage discharging.

#### 4.1.3. Simulation with battery energy storage excessive discharged

As is shown in Fig. 10, at 2.2 s, the voltage of DC bus is transited from layer 2–5, supported by the discharging of battery energy storage. At 5.8 s, a rapid removal of L3 load is took for protecting the battery energy storage from the SOC declines reached 40%. The battery energy

storage will still be in discharge, until L2 continues to be removed after 0.05 s ( $t = 5.85$  s), and the voltage of DC bus  $U_{dc}$  transits into layer 2 of battery energy storage charging mode across layer 3 and 4 by the smoothing of the flywheel energy storage.

In the case of excessive discharge of storage batteries, the system can effectively cut off the load, maintain the stability of DC bus voltage, improve the charging and discharging environment of storage batteries, and further extend the service life of storage batteries.

## 4.2. On-grid

### 4.2.1. Simulation in general pattern with PQ control

The AC bus is equivalent to a load when it is adopted PQ control strategy on-grid, the situation of which is the same as off-grid, so that only one EV pile is opened for the normal operation of charging station, at this time. When connected to the grid, the PQ control tracks the power output control signal quickly, with fast response and high stability. At the same time, the influence of the control on the frequency of the network side system is also small, and the error fluctuation is within the allowable range (not more than 1%), indicating the validity and reliability of the PQ control strategy.

The main AC/DC converter is used PQ control to send constant power to the AC side, with the reactive power constant 5kvar, active power and parameters changes as the same as the ones of case 1. As results is shown in Fig. 11, the operation of this mode is similar to the off-grid general pattern.

#### 4.2.2. Simulation with charging of the hybrid energy storage

When system is on-grid, the AC load L2 and L3 are supplied by the main power grid, so there is only L1 supplied by DC bus. With four EV piles opened at this situation, results of simulation are shown in Fig. 11. At 0.2 s, the simulation begins with  $P_{PV} = 20$  kW,  $P_L = 5$  kW, and  $P_{EV0} = 14.4$  kW. The battery energy storage system is charged with 15 A current, and flywheel charged with constant power of 5 kW. The  $P_{AC}$  is below zero, which means the voltage  $U_{dc}$  of DC bus is just maintained by the main AC/DC converter through supplying power from AC- side, and works at layer 4. At 2.2 s,  $P_{PV}$  is reduced to 10 kW,  $U_{dc}$  declines slightly and continues to work at the 4th layer.

At 4.2 s,  $P_{PV}$  becomes 5 kW, and  $P_{EV0}$  rises to 21.6 kW. The remaining power needed of the load is more than the main AC/DC converter can supply, so the hybrid energy storage system is switched to maintain the power balance of DC bus, with the flywheel smoothing and the current of battery is 0A due to the voltage of DC bus is still at the 4th layer. At 8.2 s,  $P_{PV}$  picks up to 10 kW,  $P_{EV0}$  becomes  $-21.6$  kW as discharge, and the hybrid energy storage system is changed to be continued in charge, before long the battery and flywheel motor achieve goals of SOC and speed  $n$  respectively to be standby. The voltage of DC bus changes slightly, and continues to work in the layer 3 and 4.

Hybrid energy storage system can effectively control charging under on-grid mode. Combined with the change of its control strategy and bidirectional AC/DC converter, the voltage balance of DC bus can be further maintained.

#### 4.2.3. Simulation with discharging of the hybrid energy storage

As is shown in Fig. 13, at 0.2 s, the battery energy storage is in discharge with SOC more than 70%, and flywheel in discharge with speed greater than 8000 r/min, the voltage of DC bus works at layer 3. At 4.2 s,  $P_{PV}$  becomes 20 kW,  $P_{EV0}$  is changed to  $-21.6$  kW, as the hybrid energy storage system is switched to maintain the power balance of DC bus. The battery is charged to maintain the voltage of DC bus after it rising into the layer 2 under the power smooth control of flywheel. At 8.2 s,  $P_{PV}$  is reduced to 15 kW, and  $P_{EV0}$  becomes 21.6 kW, the voltage of DC bus enters into layer 4, and the hybrid energy storage system is changed to be continued in charge. Battery and flywheel energy storages stop discharging successively after reaching the targets of SOC and speed.

As can be seen from Figs. 8–13, the DC micro-grid of EV charging station is well controlled during various cases of operation, and the proposed hierarchical coordination control strategy is satisfactory.

## 5. Conclusion

In this paper, the basic structure of the PV power DC micro-grid and its corresponding control strategy are universal. The hierarchical coordinated control of the hybrid energy storage of the flywheel and the battery has obvious effect on the smooth transition of the DC bus voltage, which can improve the power quality of the micro-grid system, and conducive to the coordinated control between the converters and the improvement of the service life of the electrical equipment in the system. They have good reference and practical value for the access and on-site consumption of new energy, as well as the interaction between EVs and the grid. Central control needs to be set to further improve system control performance, in order to ensure the reliable operation of the system, including the realization of power monitoring, convenient for the scheduling management of the charging station.

This article only concentrates on the overall structure design and

coordination control analysis of the charging station, so the future work can focus on its engineering construction and quantitative specifications. The use of the flywheel in the hybrid system has yet to be expanded. For example, when the battery cannot maintain the power balance of the system, the flywheel is further supported as a bus voltage.

## Conflict of interest

The authors declare that they have no known competing financial interests or personal relationships that could have appeared to influence the work reported in this paper.

## Acknowledgments

This work was supported by National Natural Science Foundation of China (61304134), Key Science and Technology Plan of Shanghai Science and Technology Commission (14110500700), Shanghai Key Laboratory Power Station Automation Technology Laboratory (13DZ2273800).

## References

- [1] M. Tabari, A. Yazdani, Stability of a dc distribution system for power system integration of plug-in hybrid electric vehicles, *IEEE Trans. Smart Grid* 5 (5) (2014) 2564–2573.
- [2] S. Shongwe, M. Hanif, Comparative analysis of different single-diode PV modeling methods, *IEEE J. Photovoltaics* 5 (5) (2015) 938–946.
- [3] S. Gao, K.T. Chau, C. Liu, D. Wu, C.C. Chan, Integrated energy management of plug-in electric vehicles in power grid with renewables, *IEEE Trans. Veh. Technol.* 63 (7) (2014) 3019–3027.
- [4] T. Zhang, X. Chen, Z. Yu, X. Zhu, D. Shi, A Monte Carlo simulation approach to evaluate service capacities of EV charging and battery swapping stations, *IEEE Trans. Inf. Inf.* 14 (9) (2018) 3914–3923.
- [5] M.H. Amini, M.P. Moghaddam, O. Karabasoglu, Simultaneous allocation of electric vehicles' parking lots and distributed renewable resources in smart power distribution networks, *Sustain. Cities Soc.* 28 (2017) 332–342.
- [6] Mohammadi Ali, Bahrami Shahab, An Overview of Future Microgrids, Springer Nature Switzerland AG, 2019, pp. 1–6.
- [7] L. Xiong, W. Peng, C.L. Poh, A hybrid AC/DC microgrid and its coordination control, *IEEE Trans. Smart Grid* 2 (2) (2011) 278–286.
- [8] T. Dragicevic, J.M. Guerrero, J.C. Vasquez, D. Skrlac, Supervisory control of an adaptive-droop regulated DC microgrid with battery management capability, *IEEE Trans. Power Electron.* 29 (2) (2014) 695–706.
- [9] J. Chi, W. Peng, X. Jianfang, T. Yi, F.H. Choo, Implementation of hierarchical control in DC microgrids, *IEEE Trans. Ind. Electron.* 61 (8) (2014) 4032–4042.
- [10] X. Lu, K. Sun, L. Huang, X. Xiao, J.M. Guerrero, Dynamic load power sharing method with elimination of bus voltage deviation for energy storage systems in DC micro-grids, *Proc. CSEE* 33 (16) (2013) 37–46.
- [11] B. Li, H. Bao, L. Guo, Strategy of energy storage control for islanded microgrid with photovoltaic and energy storage systems, *Autom. Electr. Power Syst.* 34 (3) (2014) 8–15.
- [12] Y. Zhang, L. Guo, H. Jia, C. Wang, An energy management method of hybrid energy storage system based on smoothing control, *Autom. Electr. Power Syst.* 36 (16) (2012) 36–41.
- [13] O. Ozel, K. Shahzad, S. Ulukus, Optimal energy allocation for energy harvesting transmitters with hybrid energy storage and processing cost, *IEEE Trans. Signal Process.* 62 (12) (2014) 3232–3245.
- [14] J.W. Shim, Y. Cho, S.-J. Kim, S.W. Min, K. Hur, Synergistic control of SMES and battery energy storage for enabling dispatchability of renewable energy sources, *IEEE Trans. Appl. Supercond.* 23 (3) (2013) 3547–3552.
- [15] T.A. Taj, H.M. Hasanien, A. Alolah, S.M. Mueen, Transient stability enhancement of a grid-connected wind farm using an adaptive neuro-fuzzy controlled-flywheel energy storage system, *IET Renew. Power Gener.* 9 (7) (2015) 792–800.
- [16] J. Goncalves de Oliveira, H. Schettino, V. Gama, R. Carvalho, H. Bernhoff, Study on a doubly-fed flywheel machine-based driveline with an AC/DC/AC converter, *IET Electr. Syst. Transp.* 2 (2) (2012) 51–57.
- [17] Q. Xiong, Y. Liao, J. Yao, Active power smoothing control of direct-driven permanent magnet synchronous wind power generation system with flywheel energy storage unit, *Autom. Electr. Power Syst.* 33 (5) (2013) 97–105.
- [18] S. Liu, H. Sun, M. Gu, J. Wen, Novel structure and operation control of a flywheel energy storage system associated to wind generator connected to power grid, *Trans. China Electrotech. Soc.* 27 (4) (2012) 248–254.
- [19] T. Dragicevic, S. Susic, J.C. Vasquez, J.M. Guerrero, Flywheel-based distributed bus signalling strategy for the public fast charging station, *IEEE Trans. Smart Grid* 5 (6) (2014) 2825–2835.
- [20] Y. Zhang, Y. Xu, H. Guo, X. Zhang, C. Guo, H. Chen, A hybrid energy storage system with optimized operating strategy for mitigating wind power fluctuations, *Renew. Energy* 125 (2018) 121–132.